Spring 2019

Experimental Study of Free-Solution Separation Under Pulsed Electrophoresis in Microchip

Xin Liu

EXPERIMENTAL STUDY OF FREE-SOLUTION SEPARATION UNDER PULSED ELECTROPHORESIS IN MICROCHIP

by

Xin Liu

Bachelor of Science
Dalian Nationalities University, 2011

Submitted in Partial Fulfillment of the Requirements

For the Degree of Master of Science in

Biomedical Engineering

College of Engineering and Computing

University of South Carolina

2019

Accepted by:

Guiren Wang, Director of Thesis

Chang Liu, Reader

Cheryl L. Addy, Vice Provost and Dean of the Graduate School

DEDICATION

I dedicate my research and thesis to my parents. They are the best parents ever, who always encourage me to overcome the challenges and provide me a chance to talk with the world.

To my soccer teammates, who share the great passion with me in the pitch and celebrate the big honor as a winner.

I also want to dedicate my work to the national parks I visited. The beautiful landscapes digest my anxiety and make me relax.

ACKNOWLEDGEMENTS

I would like to thank my advisor, Dr. Guiren Wang, for all the support and patient on my study of master's degree. Thanks Dr. Chang Liu for being my thesis reader and supporting my work.

I also appreciate the all my lab mates and staff in our department for their delicate work and assistance in the years we spent together.

ABSTRACT

Microchip electrophoresis (MCE) is a promising analytical tool started more than two decades. With the characteristics of short analysis time, trace level sample, high-throughput and easily integration, lots of efforts have been done with the transportation of the applications from capillary to microfabricated devices. However, with the complex designs on microchip rather than a single straight capillary channel, the strategies and approaches have to be figured out under the challenges of sample introduction, the improvement of separation conditions and the detection, for instance.

In miniaturized microchip, the separation channel is reduced to several centimeters or less, fast and quality separation is the priority in a very short effective distance. Compared with the results of incomplete separation of three fluorescent dyes in DC field, we modify the applied electric field by adding a short time of backward voltage to form a pulsed electric field which is inspired from the method of increasing the residence time of analytes by control the bulk flow velocity in a capillary (Kar & Dasgupta, 1999). The results show that the mixture is separated efficiently with three peaks in short distance. After the optimization of the condition of the pulsed field, the highest resolution can reach to 1.28 and 0.94 between two adjacent peaks. A longer traveling time in pulsed field is not caused the large decreasing of signal-to-noise ratio (SNR) in pulsed field as well.

Moreover, miniaturized analytical devices suffer from poor detection due to the small volume and low concentration sample. Therefore, an on-line sample pre-

concentration through stacking anion species using electrophoretic method is also investigated. There are almost 4-fold increase on signal intensity in both DC and pulsed field with sample stacking over the cases without sample stacking. In the meanwhile, the comparison of sample stacking between DC and pulsed field is made. The results illustrate that the SNR in pulsed field is 25% higher than the one in DC field.

TABLE OF CONTENTS

LIST OF TABLES

LIST OF FIGURES

LIST OF SYMBOLS

A	Absorbance
c	Concentration of the species.
l	Optical path length
ϵ	Molar absorptivity
μ_{ep}	Electrophoretic mobility
μ_{EOF}	Electroosmotic mobility
q	Charge of particle
E	Electric field strength
η	Viscosity
r	Radius
v_{ep}	Electrophoretic velocity
v_{EOF}	Velocity of electroosmotic flow
ζ	Value of zeta potential
ε	Dielectric constant
μ_{obs}	Observed mobility
w_{hi}	Peak width at half the height of the peak
R	Resolution
σ	Standard deviation of background noise
I	Peak intensity above the mean noise

LIST OF ABBREVIATIONS

B ..... Buffer

BGE ..... Background Electrolyte

BW ..... Buffer Waste

CE ..... Capillary Electrophoresis

COP ..... Cycloolefin Polymer

DCF 2,7-Dichlorofluorescein

ECD ..... Electrochemical Detection

EDL ..... Electric Double Layer

EK ..... Electrokinetic

EOF ..... Electroosmotic Flow

FASS ..... Field-Amplified Sample Stacking

FL ..... Fluorescein Sodium

ITP ..... Isotachophoresis

LIF ..... Laser-Induced Fluorescence

LOC ..... Lab-on-a-Chip

LOD ..... Limitation of Detection

MCE ..... Microchip Electrophoresis

PAD ..... Amperometric Detection

PDMS ..... Polydimethylsiloxane

PMMA ..... Polymethylmethacrylate

RB ..... Rhodamine B

S .....Sample

SNR.....Signal-to-Noise Ratio

SPE..... Solid Phase Extraction

SW.....Sample Waste

T_b.....Backward Time

T_f .....Forward Time

V_b .....Backward Voltage

V_f..... Forward Voltage

μ-TAS ..... Micro- Total Analysis System

CHAPTER 1

INTRODUCTION

1.1 General electrophoresis

The increasing demands of rapid and efficient analytical systems for separation, identification and quantification are still attracting huge attentions in many fields. In 1807, the electrokinetic (EK) phenomenon was first observed by Reuss, who noticed that clay particles migrated in water under constant electric field. In 1937, Arne Tiselius designed a new apparatus for electrophoretic analysis of charged colloidal mixtures (Tiselius, 1937). Since then, electro-osmosis and electrophoresis has been studied as two common electrokinetic effects. Nowadays, there are many types of analytical techniques for options including liquid and gas chromatography, extraction, mass spectrometry and electrophoresis. Capillary electrophoresis (CE), as one typical application of electrophoresis, is widely used in laboratory which is applicable for analytes ranging from small ions to large biomolecules such as DNA and protein (Carle & Olson, 1984; Gao, Yin, & Fang, 2004; Han & Singh, 2004; Perez-Ruiz, Martinez-Lozano, Sanz, & Bravo, 1998; J. Zhang, Das, & Fan, 2008). With the advantages of its high theoretical plate number, short analysis time and small reagents consumption, many capillary-based varieties of techniques are also being developed and playing an important role, for instance, in the completion of the human genome project and some other fields including clinical diagnosis, environmental analysis, agriculture, forensics, explosives and food analysis (Cifuentes, 2006; Pumera, 2006; Verpoorte, 2002). Meanwhile, as the emerging

of microfabricated devices, CE on microchip may lead to the new trend in analytical techniques.

1.2 Microfluidics

Microfluidics is not only the science of manipulating and controlling the fluids, usually in the range of microliter (10^{-6}) to picoliter (10^{-12}) in networks of channels with the dimensions from tens to hundreds of micrometers small amounts of fluids, but also a technology of manufacturing miniaturized devices(Whitesides, 2006). The applications of microfluidics exist more than expected. In cell biology, for example, microfluidic device could help the study of cell attachment (Lu et al., 2004) or cytoskeleton (Takayama et al., 2003). In droplet microfluidics, it can be an important tool of encapsulation for drug delivery. There are some other fields which are also combined such as optics and electrochemistry. There is no doubt that to take the advantage of microfluidics in electrophoresis will experience many benefits.

1.2.1 Micro-total analysis system

The concept of micro-total analysis system (μ-TAS), also known as "Lab-on-a-Chip" (LOC) was introduced by Manz (Manz, Graber, & Widmer, 1990). Capillary electrophoresis on microchips or microchip electrophoresis (MCE) has drawn a great interests and shown the huge potential to lead the next revolution in chemical analysis (Yin & Wang, 2005). Compare with the early separation system designed by Hjerten, the large space was necessary because of the connection between large size of power supply and detection equipment and the carriage with a long capillary immersed in the electrode vessels (Jacobson, Hergenroder, Koutny, Warmack, & Ramsey, 1994). The later work then started to use smaller size capillary for the reason of eliminating convection issues

and simplifying the instruments system. It was until the advent of microfabricated device, researcher realized the potential capability of miniaturized system in analysis. Especially the first microfluidic chip was successfully fabricated and completed the separation using a planar glass substrate (Harrison, Manz, Fan, Luedi, & Widmer, 1992). It accelerated the possibility of executing separation in an integrated device. Based on the design of the microchip, it may easily cope with hundreds of samples simultaneously in a matter of minutes or less (Ríos, Zougagh, & Avila, 2012). Thus, so many publications have done to combine the current techniques to microfluidic platform.

1.2.2 Miniaturized system

Miniaturization is an avoidable step for many aspects in modern society such as the computer, cell phone and electronic chip. The concept of μ-TAS provides the possibility to integrate several discrete processes into a simple designed device. These include sample preparation, reagent mixing, sample injection, separation and detection (Reyes, Iossifidis, Auroux, & Manz, 2002). It offers so many advantages. The less reagent consumption makes it possible for the very precious and rare analyte. Small scale of channel size will not only reduce the analysis time but also enhance the duration of high voltage (Tabuchi, Kuramitsu, Nakamura, & Baba, 2003). Moreover, the geometric pattern of multiple channels allows to carry out parallel experiments at the same time (Dunsmoor, Sanders, Ferrance, & Et Al., 2001). Many conventional applications start to transfer onto microchip platform (Nuchtavorn et al., 2013). Since the characteristics of capillary are common to the microchannel, the introduction of CE to microchip is fit it very well. Chan et al. designed a system where a liquid chromatography was plated into a

microchip to separate two dyes and biopolymers (Chan, Danquah, Agyei, Hartley, & Zhu, 2014).

1.2.3 Problems

Several advantages of miniaturization are mentioned, but there are some typical intrinsic drawbacks that MCE is also inherited from CE. One major problem is the limitation of detection (LOD) (Colyer, Mangru, & Harrison, 1997). According to Beer-Lambert law (Beckers & Bocek, 2000):

$$A = \epsilon c l \qquad (1)$$

Where A is the absorbance (AU), ϵ is the molar absorptivity ($dm^3mol^{-1}cm^{-1}$), c is the concentration of the species, and l is the optical path length (cm). Since the depth of the microchannel is very short (it is only 50 μm in our microchip) and the sample at trace level contributes to the concentration in order of 10^{-6} M, it is not difficult to get a conclusion that an improvement of sensitive detection is needed. Currently, there are many detection methods which can be coupled with MCE including laser-induced fluorescence (LIF), electrochemical detection (ECD) and pulsed amperometric detection (PAD) (G. Chen, Lin, & Wang, 2006; Vickers & Henry, 2005).

Sample pre-concentration is another technique to enhance the detection sensitivity (Karlinsey, 2012). The purpose is to concentrate low concentration sample prior to analysis. Instead of off-line sample preparation, the sample in the integrated system can be detect right after the preparation which attributes less chance of the contamination during the process of transfer. Here are three most representative methods: field-amplified sample stacking (FASS), isotachophoresis (ITP) and solid phase extraction (SPE) (Bharadwaj & Santiago, 2005; Herrera-Herrera et al., 2011; Lee & Mems, 2011).

1.3 Microchip-based platform

As the development of microfabricated technology, a variety of materials are used to produce size-reduced microchip in the range of several centimeters shown in Figure 1.1. The common materials include quartz, glass and some polymers such as polydimethylsiloxane (PDMS)， polymethylmethacrylate (PMMA) and cycloolefin polymer (COP) (Kim, Cho, Lee, & Kim, 2005; Köhler et al., 2012). The simple design of microchip is the cross geometry which consists of two straight microchannels to form an intersection. There are four reservoirs on each end of the microchannel as the function of container of loading sample and buffer. Thus, the next question is how to control the fluid flowing in the channel efficiently.

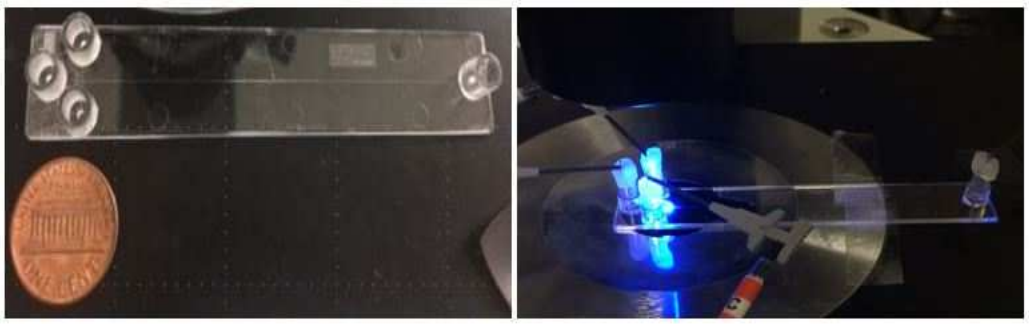

Figure 1. 1 A microfluidic chip performing the electrophoresis.

1.3.1 Electrokinetic control

To have a high performance of separation efficiency on microchip, the introduction of sample is the fundamental step which must be steady and repeatable for each run. In conventional CE, the sample could be introduced into capillary by placing the inlet into a sample vial via capillary action, pressure, siphoning, gravity or electrokinetically. Considering the extra pump instrument needed to connect with the

microchip and hard volume control with pressure in a micrometer channel, EK injections are predominant way as it can easily generate flow motion by setting the potential to each reservoir. Sometimes the sample loading and injection are performed by combination of pressure driven and EK forces (Karlinsey, Monahan, Marchiarullo, Ferrance, & Landers, 2005; L. Zhang, Yin, & Fang, 2006).

Despite an electrophoretic bias was reported during the pinched injection that the neutral species were injected more than anionic species with fixed amount of volume in the area of the intersection (Jean P. Alarie, Jacobson, & Michael Ramsey, 2001), this bias can be overcome by implementing gated injection or having longer injection time. And several researchers developed some new designs to avoid the bias during sample injection (Bharadwaj, Santiago, & Mohammadi, 2002; Shultz-Lockyear, Colyer, Fan, Roy, & Harrison, 1999). The details about the operation of EK gated injection will be discussed in chapter 2.

1.3.2 Electroosmotic flow

Electroosmotic flow (EOF) is playing an important role when the channel size comes to the level of micrometer or nanometer. It is the special force to drive the motion of the entire liquid filled in the channel under the electric field as shown in Figure 1.2.

In CE, due to the dissociation of silanol group (Si-OH), the inner wall of a capillary becomes a negatively charged surface where a bunch of the cations are attracted to form the electric double layer (EDL). The first layer is called Stern layer where the cations are absorbed tightly from the liquid. Meanwhile, the second layer consists of positive ions compensated to surface charges via Coulomb force, which are not rigidly held but tend to move around out of the first layer and extend to bulk flow gradually. It is

called “diffusion layer”. Beyond the EDL, the number of cations is equal to the one of anions. Once an electric field is applied, only the cations in diffusion layer start to move toward the cathode and the bulk flow then is dragged along with them in the same direction. This phenomenon is electroosmotic flow. It also can be generated on different material in MCE (Nuchtavorn, Suntornsuk, Lunte, & Suntornsuk, 2015).

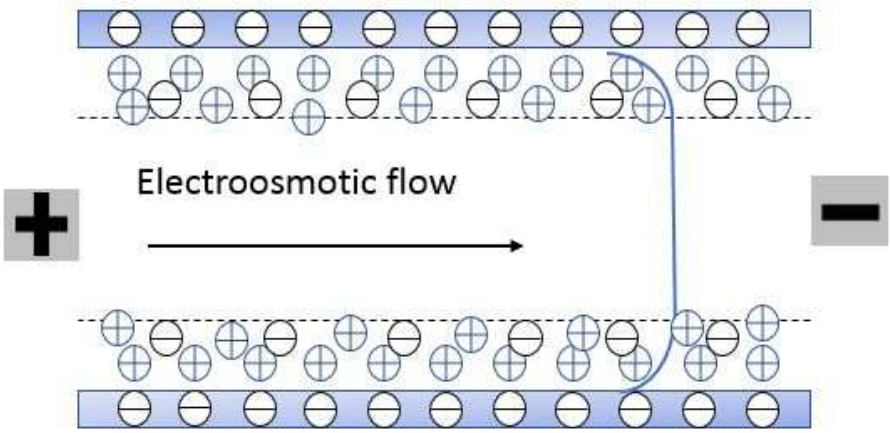

Figure 1. 2 Schematic drawing of the electroosmotic flow (EOF) in microchannel where EDL formed on the surface.

Furthermore, an important character of EOF is the profile pattern which is flat, compared with parabolic profile caused by pressure. The profile or “plug flow” caused by EOF is preferred because of its uniform distribution of driving force along the channel, which could minimize the band broadening (Haswell, 1997).

1.3.3 Visualization

The total length of a microchip is designed to several centimeters compared with the traditional capillary as well as the diameter of the channel can be 50 μm or less. Then, the separation time is further reduced than the one in CE. Jacobson reported that a binary mixture was separated in glass microchip for sub-millisecond (Jacobson, Culbertson,

Daler, & Ramsey, 1998). Since the process in capillary is invisible, there is less opportunity can be handled when an unexpected situation occurred. However, it is possible to observe the whole separation process in microchip under the microscope and record using CCD camera. For example, the research of enhancing the sensitivity of sample injection, the stacked analyte can be easily visualized under camera (Wuethrich & Quirino, 2017). Especially, the process of injection is whether successfully completed or the performance of the separation is occurred which can be observed. Therefore, based on the real time observation, it provides the evidence for the optimization of the condition of sample injection and separation (Ueda et al., 2001).

1.3.3 Challenges

The length of channel required to separate two analytes in CE is directly proportional to the initial length of the sample. The big change platform from long capillaries to short length microchannels on a microchip brings some benefits as well as challenges. In general, the size of a microchip down to several centimeters which allow the ultra-small sample plugs and short separation path to be able to have fast analysis and separation with less diffusion. But what application is exactly fit for it? In fact, it depends on the application. It is critical to know that the real advantage of EK injection is the flexibility based on the pattern of the chip, voltage range, desired sample size and the target analytes. A decent example is the analysis of single cell in microfluidic devices (Breadmore, 2012; P. Chen et al., 2010; W. H. Huang, Ai, Wang, & Cheng, 2008). If the selectivity of the mixture is constant, short path length is reasonable because the resolution is proportional to the square root of the migration length when no other parameter is considered (Dolník, Liu, & Jovanovich, 2000).

However, the short separation length raises an issue of the injection of the sample length. If the sample plugs are too broad which may cause an incomplete separation but a gain in sensitivity; shorter plugs may result in the limitation of detection (Bruin, 2000). The length of the plug can be adjusted by programmed power supply or pressure (Blas, Delaunay, & Rocca, 2008; Ermakov, Jacobson, & Ramsey, 2000; Palmer, Burgi, Munro, & Landers, 2001). Also, the separation voltage can be modified based on the mobility of the analytes (Blas, Delaunay, Ferrigno, & Rocca, 2007). An important reference of sample length injected into channel and the appropriate separation voltage has to be studied before fabricating and performing the separation on a miniaturized microchip (McDonald et al., 2000).

1.4 Application of Pulsed field

The application of pulsed field can date back to the paper reported by Schwartz that large yeast chromosome DNA up to 2000 kb can be separated in gel electrophoresis whereas large DNA usually stay and move together at constant electric field (Schwartz & Cantor, 1984). Birrer showed that the pulsed field could influence the migration pattern of large DNA molecules in the sieving matrix (Birrer, Simon, & Lai, 1990). On the contrary to the long time gel preparation and separation, pulsed field gel electrophoresis has also carried out on microchip (Backhouse, Gajdal, Pilarski, & Crabtree, 2003; Lin, Wang, & Fu, 2008). Another application of pulsed field was introduced in the field of food analysis. For example, it can be used to break down cell membrane and more information is covered in this review (Soliva-Fortuny, Balasa, Knorr, & Martín-Belloso, 2009).

As mentioned above, knowing that in a miniaturized microchip the length of separation channel is becoming an important parameter. Taking advantage of short separation length to acquire high separation efficiency and resolution is the key for any application in a microchip. In traditional method, usually one way to enhance the resolution is that to have a longer separation length (Kutter, 2000). However, it may not be a practical way to extend to the desirable length in current equipment. Even though it is applicable, it will be a challenge to provide proper voltage or pressure to maintain the steady migration of analytes across the whole length because of the gradient induced by concentration, pH or pressure (Bharadwaj & Santiago, 2005; Sinton, Ren, Xuan, & Li, 2003). Moreover, a large-size apparatus goes against the conception of miniaturization. The other one is to increase the electric field strength. But extremely high voltage will not only result in Joule heating effect but also breaking down the material. And high voltage will create fast EOF which may result in poorly separation between two similar analytes. Either one seems not quite a good strategy for separation and resolution if the effective separation length is limited. Therefore, a simple and effective method needs to be seeking that an electric field with appropriate recycle period could slow down the migration speed to meet the request for extending the residence time. The different mass-to-charge ratio of the analytes under pulsed field also give a chance to complete the separation. This method will not introduce additional instruments to current system which is favorable.

1.5 Objective of thesis

Microfluidic electrophoresis separation now has been a powerful alternate method because there are many advantages over conventional analytical applications. The improvement and optimization are always being exploring in the application of analytical

technique. In CE, the polymer solution replaces the traditional slab gel as a sieving matrix provide much more accuracy selective and time-saving separation. Surface modification of the capillary is often used to suppress EOF which may have effect on electrophoretic separation and avoid the reaction between the channel surface and the sample (Buchholz, Huiberts, Stein, & Barron, 2002; Llopis, Osiri, & Soper, 2007). Moreover, the control of the bulk flow by reducing the velocity of EOF is another approach to extend the residence time of the analytes in order to improve the resolution (Kar & Dasgupta, 1999). These approaches are also suitable for microfabricated devices (Barker, Ross, Tarlov, Gaitan, & Locascio, 2000; Belder & Ludwig, 2003; Liu & Lee, 2006).

As the unique feature of miniaturization, there is a need to complete the analysis on a small microchip with short separation channel. In this study, we carry out the electrophoretic separation of a dye mixture on an untreated microchip which is made of cyclic olefin polymer (Roy, Das, & Yue, 2013). An incomplete separation is observed under DC field. Therefore, a simple and effective solution needs to be looking for. Considering the feasibility and simplicity, the modification of high-power supply without introducing extra instruments is considered as a substitute. Then we come up with an idea of using pulsed field offering proper time ratio which could achieve better separation. Thus, the aim of this study is to find an optimal condition to enhance the separation in a short effective separation length on a microchip. Both DC and pulsed field are used as the separation voltage and compared. The performance of the pulsed field is evaluated.

CHAPTER 2

THEORY

2.1 Microchip electrophoresis

Microchip electrophoresis (MCE) is a highly integrated system. It consists of a high voltage supply, microchip, light source, microscope and coupled charged digital camera. The automation of individual steps includes sample introduction, sample injection, separation and detection. The miniaturized instruments could function in a manner of reduction of space and volumes, analysis and reaction time and sensitive detection. Here, we perform the free solution electrophoresis to solve the separation problem in a fixed separation length about 4 mm on a microchip (Figure 2.1) and propose a method to modify the voltage scheme to improve the resolution as well.

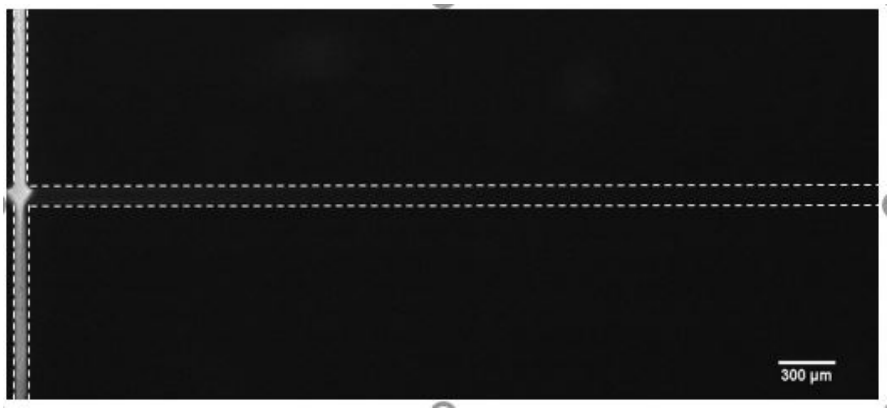

Figure 2. 1 The field observation via CCD camera with the separation distance of 4 mm from the intersection.

2.2 Pulsed electric field

In DC field, the separation voltage is only in one direction from left to right (Figure 2.1). On the contrary, a square wave form pulsed electric field is applied to drive the sample for separation shown in Figure 2.2. It consists of forward and backward voltages which are represented as V_f and V_b respectively. T_f is denoted as the duration of the time for forward voltage, and T_b is the pulse time for backward voltage.

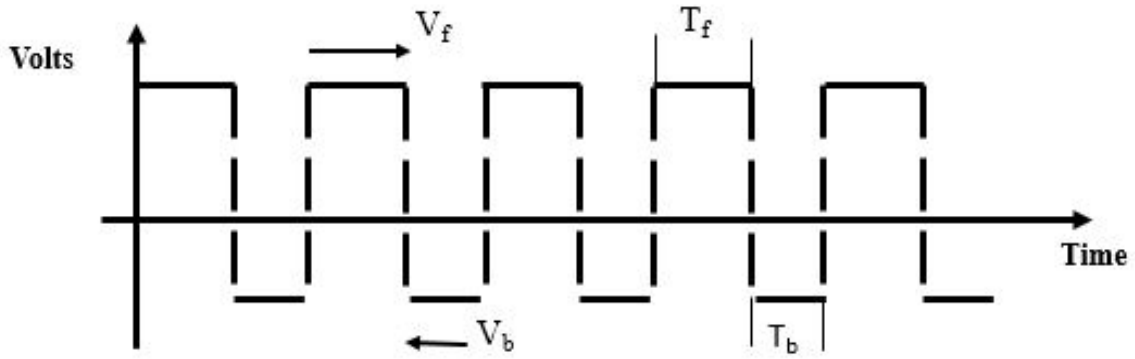

Figure 2. 2 Schematic of the square wave pulsed electric field for separation. V_f and V_b are the forward and backward voltage which are in opposite direction. T_f and T_b are the pulse duration for each, respectively.

2.2.1 Pulse ratio

An obvious character of pulsed field is the distribution of time for one recycle. In DC field, if the separation can be achieved, to improve the separation, either very high voltage or long separation channel are needed. However, the separation channel is not long enough on a microchip which may cause an incomplete separation. It is meaningful to complete the separation by finding a method in aspect of increasing the residence time. Without any additional parts, modification of voltage scheme is the easiest way to extend the residence time for the analytes. Another purpose is to reduce the observed mobility due to their different charge-to-mass ratio. After several periods, the accumulation of the

velocity difference will make the mixture separated. For example, T_f is 100ms and T_b is 50ms, the ratio will be 2:1. Make sure that the T_f cannot be too long because there will be no difference with DC field if the sample already passes by the detection point, but the period is not finished.

2.2.2 Voltage value

To apply the pulsed field, only a proper time of V_b is added to voltage program. Then the difference between voltage scheme can be easily compared. In Figure 2.2, we notice that the value of the V_f is always higher than V_b. The reason for this arrangement is to make sure that the sample plug could still move to the BW smoothly and there is not sample flowing back when the backward electric field is on after the sample injection. It is the same idea for setting the time that T_f is longer than T_b.

2.3 Migration velocity

As mentioned above, EOF is an important feature when the size of the channel is down to micro- or nano-meter. The microchip regarded as the miniaturized version of capillary shares the same mechanism in CE. The basic principle of electrophoresis can be defined as different migration velocity of the species presented by their charges under the electric field. In practical situation, the effective electrophoretic separation is affected by two parameters: the electrophoretic mobility of each analyte and the mobility of the EOF.

The electrophoretic mobility (μ_{ep}) is the response of individual ionic motion in the electric field. There are two forces, electrostatic and friction force, which are in equilibrium:

$$qE = -6\pi\eta r v_{ep} \qquad (2)$$

Noticing that the μ_{ep} is proportional to the charge (q), and inversely proportional to the radius (r) and the viscosity (η) of the circumstance which can be written as the following equation (3):

$$\mu_{ep} = \frac{q}{6\pi r\eta} \quad (3)$$

Therefore, the migration velocity is expressed as the result of the electrophoretic mobility times the electric field strength shown in equation 4:

$$v_{ep} = \mu_{ep}E \quad (4)$$

We can conclude that the charge or the size could have different selectivity of the analytes which provides the fundamental mechanism for electrophoretic separation.

The other one is EOF as mentioned early which is influencing the bulk flow velocity in the channel. The electroosmotic mobility (μ_{EOF}) is described in equation 5:

$$\mu_{EOF} = \frac{v_{EOF}}{E} = \frac{\varepsilon\zeta}{4\pi\eta} \quad (5)$$

Where ε is dielectric constant and ζ is the value of zeta potential. Compared with the electrophoretic mobility of analytes, EOF is playing a dominant role on an uncoated channel surface. Accordingly, the observed mobility (μ_{obs}) should be the sum of the ion's electrophoretic mobility and the mobility of the EOF, since the EOF is barely eliminated (Dolnik & Liu, 2005):

$$\mu_{obs} = \mu_{ep} + \mu_{EOF} \quad (6)$$

From the equation 6 (Milanova, Chambers, Bahga, & Santiago, 2011), cations move toward the cathode in the same direction of EOF flow; anions move toward the anode in the opposite to the EOF flow and the neutral analytes move as the same speed as the EOF which is used to identify the velocity of the EOF experimentally. Due to the EOF existence, all analytes can move in the same direction but with different velocity.

However, strong EOF could result in some problems such as loss of resolution, bad separation efficiency and absorption (Belder, Deege, Kohler, & Ludwig, 2002; Hu et al., 2003), surface modification can suppress and stabilize EOF. Of course, the application of pulsed field used to decrease the EOF is the approach to improve the separation in this research.

2.4 Stacking mechanism

Sample at the trace level will bring a lot of technique difficulties in detection. Two solutions could be set about overcoming the poor acquisition of the signal among the background noise. One is to develop sensitive detection methods; the other one is to stack analytes in concentration by utilizing the electrophoretic methods before detection (Giordano, Burgi, Hart, & Terray, 2012). A basic principle of anion species sample stacking is illustrated in the Figure 2.3.

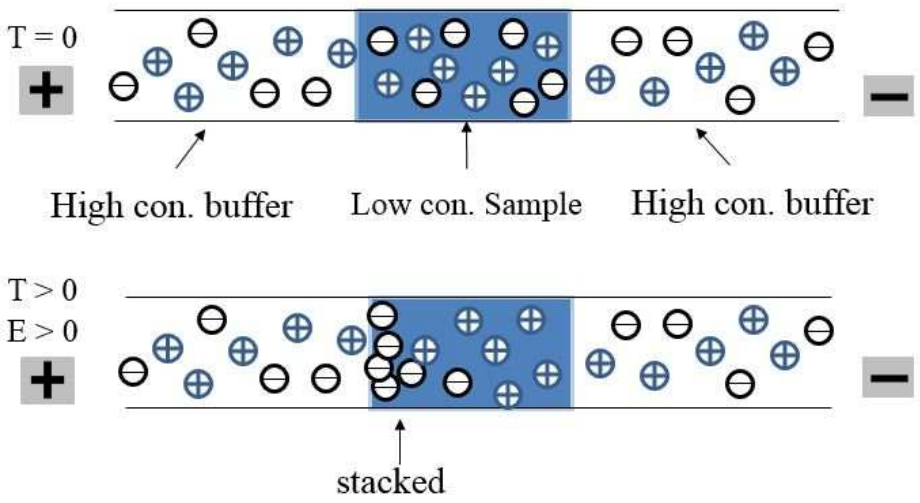

Figure 2. 3 Scheme of anion species stacking mechanism in microchannel.

When T = 0, a plug of sample prepared with low conductivity solution (i.e. DI water) is surrounded by high conductivity background electrolyte (BGE) the separation

channel. After the electric field applied, the low conductivity sample will experience the enhanced electric field and move rapidly. Once they cross the boundary into high conductivity buffer, the anion species will slow down and stack. This mode is common used for stacking in CE and MCE.

2.5 Measurements

2.5.1 Resolution

Resolution (R) can be defined as separation of centers over bolus width which is a simple way to characterize the separation of two analytes. It can be defined by using theoretical plates number in CE. Here, the resolution can be calculated in equation 2 since the two peaks are following the Gaussian distribution:

$$R = 1.18 \times (t_2 - t_1)/(w_{h1} + w_{h2}) \quad (7)$$

Where $t_2 - t_1$ is the time difference between two peaks, w_{hi} is the peak width at the half height. Based on the equation 2, the improvement of resolution can result from the increasing the residence time between two analytes or short sample plug with fast separation could reduce the band width caused by diffusion.

2.5.2 Signal-to-noise ratio

In the fluorescence detection, signal-to-noise ratio (SNR) is the parameter to show the fluorescent intensity during the separation process. The microchip is placed on the stage of the microscope. Under the 4X lens, the field with around four millimeters long channel can be monitored. The detection point is picked up at any location along the channel where the signal intensity is plotted on the axis of time scale. The SNR is defined as the peak intensity above the mean noise level (I) over the twice of the standard deviation of background noise (σ) in equation 7 (Bharadwaj et al., 2002):

$$SNR = {}^{I}/_{2\sigma} \quad (8)$$

Then the SNR can be evaluated with DC and pulsed field based on the electropherogram in each situation.

CHAPTER 3

EXPERIMENTIAL MATERIAL AND METHOD

This chapter describes the setup and experimental procedures that shows the connection of the system and the capability of miniaturization for a planar microfluidics chip in the performance of separation. Gated injection is used to create sample plug to separation channel. The separation conditions are investigated and compared by applying continuous and pulsed electric field.

3.1 Chemicals and reagents

There are three dyes used in this research: 50 μM rhodamine B (RB) with molecular weight 479.02 is neutral (0) which are purchased from Fluka. Two negatively charged dyes are fluorescein sodium salt (FL) (-2) from Sigma-Aldrich and 2,7-Dichlorofluorescein (DCF) (-1) Acros Organics with the concentration of 20 μM and 75 μM with the molecular weight 376.28 and 401.20, respectively. 1M solution of Sodium hydroxide (NaOH) from Merck is prepared to rinse and clean the microchip before or after the experiments. 1 mM sodium chloride (NaCl) and 0.5 mM HEPES buffer (pH = 7.5) are prepared and diluted with DI water. Then flushing with DI water right way to avoid the damage of the channel surface. Ethanol (sigma) is used to dissolve the powder of DCF and diluted with DI water. The RB and FL are soluble and prepared with DI water directly. All buffer and solutions are filtered through a cellulose syringe filter with 0.2 μm pore size before use. All chemicals are used without further treatment.

3.2 Experimental setup

The setup in this experimental study is shown as Figure 3.1. A microchip is placed on the stage of the microscope. There are four reservoirs where each of them is covered with a female Luer interface holder lid. And four holders can stabilize the electrodes. A high voltage sequencer 448LC 6000 (Labsmith, USA) connected with four platinum electrodes to each reservoir provides the programmed voltage through high voltage cables. An inverted epifluorescence microscope (Olympus IX70) coupled with a CCD camera under 4X lens is used to monitor the microchannel and record images sequence. A 4 mm length of the separation channel can be observed for separation. A light source (X-Cite 120 illuminator, EXFO) provides blue light to excite the fluorescent samples. The images sequence is further processing using Origin software to get the electropherograms.

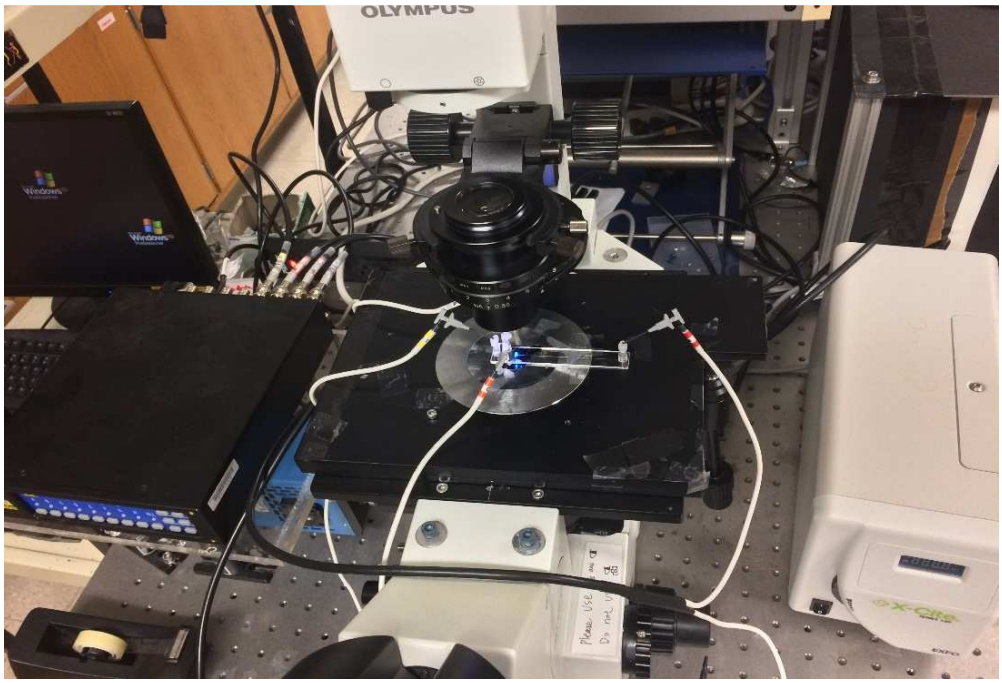

Figure 3. 1 The experimental setup of microchip electrophoresis.

3.3 Microchip introduction

A commercial microchip made with cyclic olefin polymer (zeonor) was purchased from Microfluidic Chipshop (Germany) as shown in Figure 3.2.

Figure 3. 2 Schematic layout and dimensions of the microchip. The total length 87 mm from B to BW; 5 mm from S and SW to the intersection. The depth and width of the channel are 50 μm.

The layout of microchannel consists of two straight channels to form a cross intersection. There are four reservoirs which are sample (S), sample waste (SW), buffer (B) and buffer waste (BW), respectively. The channel is 50 μm in both depth and width. The total length from B to BW is 87 mm and it is 10 mm from S to SW.

To produce a cheap, durable and functional microchip is still in progress. Now several materials have been studied and used for fabrication as a substrate, such as fused quartz (Jacobson, Moore, & Ramsey, 1995), glass (F.-C. Huang, Liao, & Lee, 2006), and some polymers (Duffy, McDonald, Schueller, & Whitesides, 1998; Hu et al., 2003; Jena & Yue, 2012; Kim et al., 2005; Wang et al., 2002). The characteristics of these materials will have different surface properties which may heavily cause the various consequences of the separation efficiency (McDonald et al., 2000). In some cases of biomolecular analysis, the interaction between sample and wall and the surface heterogeneity may result in the loss of sample and poor electrophoretic separation. Therefore, it is essential to understand the performance of a new chip. The popular approach is the surface

modification which aims to avoid the absorption from the wall and to suppress the EOF to reduce the band broadening due to nonuniform surface charges.

3.4 Voltage control

The applied voltage has a great impact on migration time and the quality of the separation. Even the small size channel has an advantage of quick heat dissipation, extremely high voltage is not encouraged. A doable voltage needs to be compatible with the concentration and composition of analytes, the material of chip and the separation length of the microchannel. Then, Table 3.1 shows the voltage setting applied into MCE based on the situation in our research.

The value of the voltage of four reservoirs for each step can be easily set with the software in the computer which is connected to the high voltage sequencer. There are two ways to change the steps either pressing the button on the panel by manual or switching automatically by giving the desired time in software. Since the time to wait for the sample loading of each experiment is different, we choose to manually switch the loading step to the next and the rest of steps will be completed automatically.

In DC field, only one direction of the electric field is on which is forward in the Table 3.1. For the accuracy, the company suggest that the voltage is better crossing the zero. The value of 1500 V, 2500 V and 3500 V are programmed on the reservoir of B and BW. As mentioned above, one period of the puled field consists of a proper time of forward and backward voltage. Because the separation length is limited, longer T_f will drive the sample flow as the same way as it goes in DC field during the process of sample migration.

Table 3. 1 Programmed voltage setting for four reservoirs using gated injection method in three steps of separation under DC field (1500 V, 2500 V and 3500 V); 800 V backward voltage added for pulsed field. (Unit: V)

	S	BW	SW	B
Loading	180	450	0	150
Gating	300	-800	0	150
Forward	100	-500	100	1000 2000 3000
Backward	100	1000	100	200

3.5 sample injection methods

For the electrophoresis on a microchip, sample injection is one of the most critical steps to achieve efficient and sensitive analysis. In contrast to capillary, multiple channels are designed to complete the job instead of one. EK sample injections are widely used because of no external devices added into the system and the easy flow motion generation. In one review paper, several current injection modes are summarized (Blas et al., 2008). With the geometry of two orthogonal channels, the common modes include floating, dynamic, pinched, and gated injection. At the same time, the designs such as "double T" or more complicated patterns are also examined to confine the shape of the sample plug. (Gong, Wehmeyer, Stalcup, Limbach, & Heineman, 2007) There are two main injection methods described here: pinched and gated injection. The manner of the injection mode depends heavily on the requirement of the application.

3.5.1 Gated injection

In this study, the injection mode we have been using is gated injection. In general, it includes three independent steps: loading, gating and dispensing in Figure 3.3.

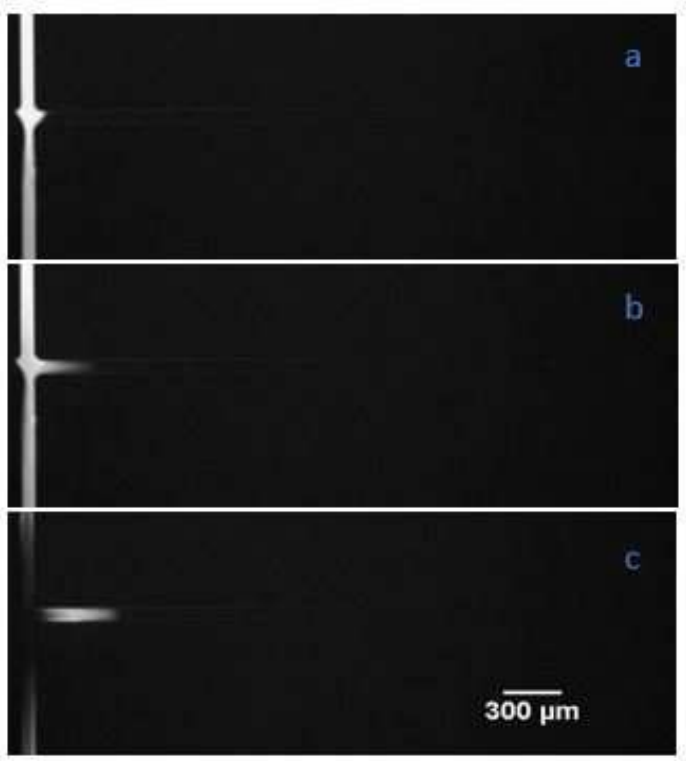

Figure 3. 3 The process of gated injection in steps of (a) loading, (b) gating, and (c) dispensing. The gated time is 300 ms.

A volume of 12 µL sample is pipetted into S reservoir. The other three fill with DI water before loading the sample. In loading step, the voltage directs the sample flow from S to SW and ensure that no sample is running into B and BW. For the horizontal channel, higher voltage applied on the end of BW, due to the long distance from the intersection, is against the one from B side to form a stable loading shape in Figure 3.3a. The sample volume around the intersection could be adjusted by balancing the voltage between B and BW (Jean Pierre Alarie, Jacobson, Culbertson, & Ramsey, 2000). In the gating step, the

sample needs to make 90 degree turn into separation channel in Figure 3.3b. One advantage of this injection is that the length of the sample plug can be changed based on the demands since the gating time is easily setting via the HVS software. To have a pull back after injection, the voltage on the S in dispensing step is smaller than in loading step. According, a reliable separation is achieved (Figure 3.3c).

Gated injection is very convenience to create a sample plug with desired length. Another advantage is the ability to inject multiple plugs at the same run which means that the second plug can be injected before the previous one is not reached to the detector yet (Büttgenbach & Wilke, 2005). The gating time in this experiment is 300 ms, and the voltage setting is as seen in Table 3.1.

3.5.2 Pinched injection

In pinched mode, there are usually two steps: a loading step and a dispensing step. After the sample is flowing steadily from S to SW, the voltage switches to the dispensing step for separation. The plug size using pinched mode is usually smaller than gated mode, but it fits for the quantity analysis since a precise volume control in loading step is determined by the intersection. Meanwhile, the detection limits of the significant low amount of analyte is obvious, but it allows a highly efficient separation. Therefore, a careful consideration between sensitivity and efficiency has to be made before implementing the injection method in analysis of diverse species (Jin, Anderson, & Kennedy, 2013).

3.6 Procedure of sample stacking

The same microchip is used in the experiment of sample stacking. The low conductivity samples are prepared within DI water. The high conductivity buffer is mixed

with 1 mM NaCl and 0.5 mM HEPES with pH 7.5. A gated injection is to create the sample plug. A sample mixture containing RB (0) and FL (-2) is to illustrate the anionic analyte stacking phenomenon.

The microchip first is rinsed with 1 mM NaOH for three times. Then flush with DI water at least three times. The HEPES buffer is loading into the channel with the syringe and 12 μL sample are added into sample reservoir.

CHAPTER 4

RESULTS AND DISCUSSION

4.1 Effect of DC field

4.1.1 Adjustment of DC field

In the beginning, four different electric field strength are employing to separate the mixture with the voltage 1000 V, 1500 V, 2500 V and 3500 V. However, the sample is keep leaking into separation channel in the situation of 1000 V shown in Figure 4.1. In gating step, a large potential difference between S and BW needs to apply in order to complete the 90-degree turn across the whole channel.

Figure 4. 1 Sample is leaking into separation channel after the sample injection is done under the separation voltage of 1000 V.

When it switches to the separation voltage, the voltage on the S is from 300 V but the B is 500 V which may not create a strong pull back. The other three cases are 1000 V, 2000 V and 3000 V on the S reservoir which can strongly push the sample away (Oleschuk & Harrison, 2003).

4.1.2 Measurement of EOF

The velocity of EOF can be measured by using fluorescent neutral marker since the mobility of neutral species is equal to EOF (Milanova et al., 2011; Preisler & Yeung, 1996). One of the samples we are using is rhodamine B (RB), though we can roughly know the velocity of EOF under the different DC field.

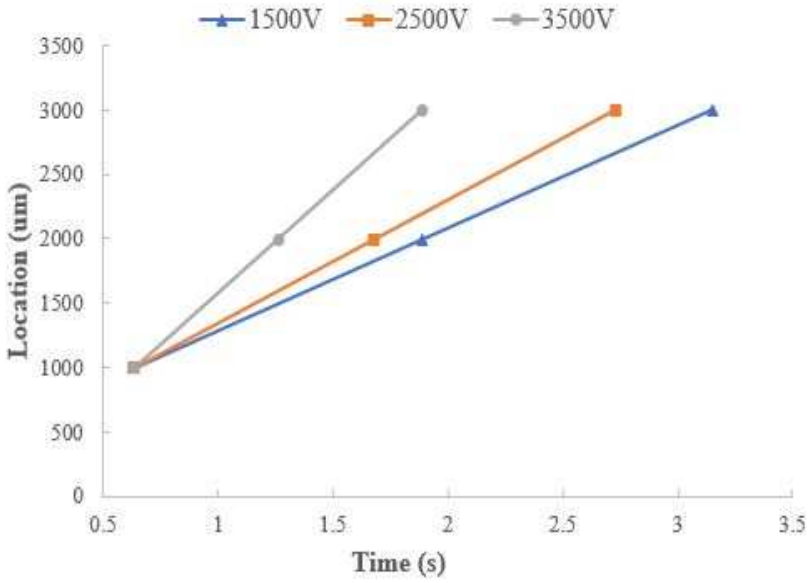

Figure 4. 2 The migration velocity of the neutral dye RB from 1mm to 3 mm under the DC field of 1500 V, 2500 V and 3500 V.

The Figure 4.2 draws the lines of the migration speed of the three. The distance to calculate the velocity is from 1000 μm to 3000 μm where the RB is moving through. We can clearly see that the high voltage results in fast mobility of analytes. In short migration pathway, the mixture may not have enough time for separation due to the close mobility. Therefore, the application of pulsed field to increase the residence time by the modification of EOF is examined.

4.2 Comparison of DC and pulsed field

4.2.1 Separation of DC and pulsed field

The mixture is made of fluorescein sodium (FL), dichlorofluorescein (DCF) and RB. First, the sample is carrying out under DC electric field with 1500 V, 2500 V and 3500 V. Then we repeat every step to run the pulsed field separation which only the backward voltage of 800 V is added in dispensing step. In pulsed field, the time distribution is 100 ms: 50 ms for forward voltage (V_f) and backward voltage (V_b) for each situation. The electropherograms is plotted in Figure 4.3. All the three bands in DC field are narrower as expected when they pass by the detection point because higher electric field strength creates high speed of EOF that results in short analysis time. However, only 1500 V shows the separation of the mixture with three peaks in Figure 4.3a. In Figure 4.3b and 4.3c, just two peaks are observed: one peak is RB; the other one is the mixture of FL and DCF. It is reasonable that the separation of neutral and negatively charged dye should be easy (Jacobson et al., 1998; L. Zhang et al., 2006). But the two negatively charged dyes are not yet separated because of the high EOF.

On the contrary, the mixture in pulsed field is travelling slower relatively because of adding 50 ms backward voltage. From the Figure 4.3, all three conditions under pulsed field shows the separation with three identified peaks, even the diffusion is introduced due to the longer traveling time. But this diffusion is not critical to affect the results considering the priority of separation in a short distance. The fact is showing that the pulsed field could enhance the separation between two close charged analytes which DC field could not. One reason is that the application of pulsed field increases the residence time for each analyte. But it is not simply only because that the pulse electrophoresis has

longer separation time. If so, we just need to reduce the electric field strength or voltage for the DC field separation. Then the second one is the accumulation of the momentum. Each analyte has its own mobility under the same electric field, but higher EOF make the μ_{obs} of each

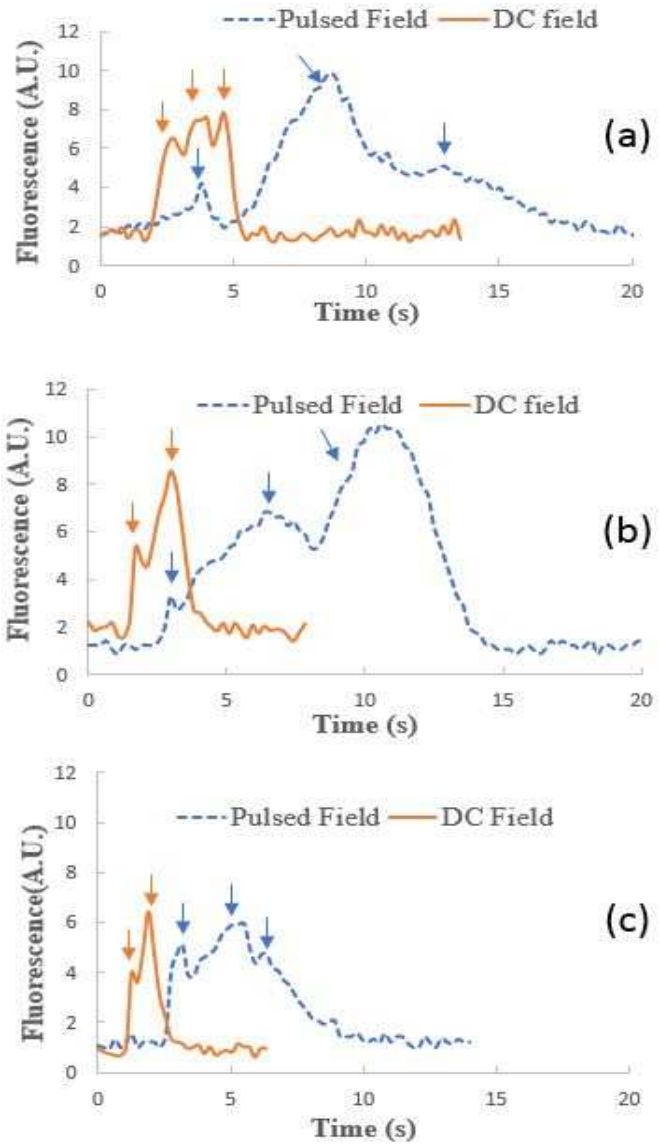

Figure 4. 3 The electropherogram of DC and pulsed electric field under (a)1500 V and 1500 V, 800 V; (b) 2500 V and 2500 V, 800 V; (c) 3500 V and 3500 V, 800 V. The time distribution is 100 ms and 50 ms for Tf and Tb in pulsed field, respectively.

analyte experience less different in DC field. However, because the sample in pulsed field experiences the process of start and stop, with the different molecular weight of each analyte the larger one will have big inertial force with its own response time. When the direction of the electric field is changed, it shows the weaker response and still moves forward. On the contrary, the other two analytes with light molecular weight have quicker response and slow down during the time of the change of the electric field. Meanwhile, some molecules response fast and some slow which is depending on their size and geometry according to the equation 9:

$$v = {F_D}/{\bar{f}} \qquad (9)$$

Where F_D is drag force, $\bar{f}$ is frictional drag coefficient which is changed with the shape of molecules. Then the interval of reaction time and the different inertia eventually results in the separation of each analyte with their own migration velocity through the alternating electric field. These are the two main possible reasons that the separation enhancement can be achieved under pulsed field.

4.2.2 SNR

The SNR for the three parallel groups above is calculated. Figure 4.3 shows that pulsed field can separate the mixture more efficient over DC field in the short effective distance. To measure the SNR, three locations are selected where the plug moves around to the downstream of 2 mm along the separation channel. At each location, the signal of the plug can be measured which the highest one is plotted in Figure 4.4. Under the condition of 1500 V in DC field in Figure 4.4a, the sample moves all the way in 3.36 s. And the SNR is decreased by 50%. Compared with DC field, the sample in pulsed field needs 6.5 s to move but the SNR is decreased by 45%. The Figure 4.4b-c shows the SNR

drop in the other two cases of DC field and pulsed field with the same condition in Figure 4.3. Because of the increasing voltage, the time for sample traveling is shorten to 2.3 s and 1.68 s in DC field with SNR drop percentage of 33% and 67%. And there are 6.3 s and 4.2 s in pulsed field with SNR drop percentage of 7% and 65%, respectively.

The SNR decrease less under the pulsed field in Figure 4.4b in the same migration distance. The DC field in three cases brings more than 50% reduction of the SNR. In general, the applied electric field could increase the diffusion rate which will cause the decreasing of the SNR (You, Be, & In, 2011). In pulsed field, since the backward voltage is added, the migration velocity is slowing down that the sample will take longer time from one location to another. Due to the long migration time, the diffusion and dispersion time of the plug is increased. Hence, the extended residence time will contribute to the drop of the SNR. If the SNR in pulsed field is dropped too much, this may not be good for the detection. However, the results show that the longer time caused by the application of pulsed field is not the main contribution to the reduction of SNR compared with high diffusion rate created by constant electric field. Moreover, the low concentration, large surface to volume ratio and the mismatch of the electroosmotic mobility between the sample and buffer may result in dilution inside the channel where an internal circulation is generated (Sinton, Ren, Xuan, et al., 2003).

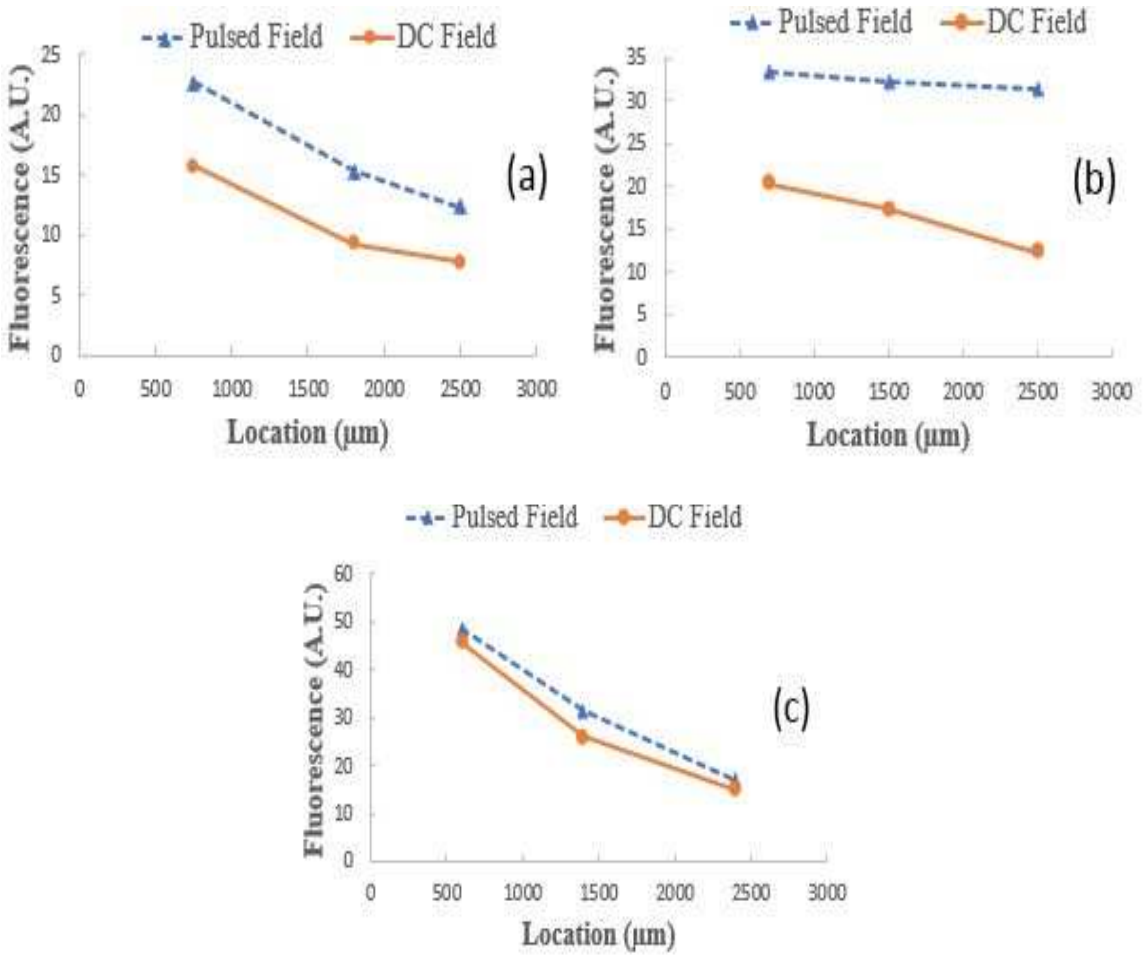

Figure 4. 4 Comparison of SNR decreasing trend between DC field and pulsed field (a) SNR drop 50% in 3.36 s with DC and 45% in 6.5 s with pulsed field; (b) SNR drop 33% in 2.3 s with DC and 7% in 6.3 s with pulsed field; (c) SNR drop 67% in 1.68 s with DC and 65% in 4.2 s with pulsed field.

4.3 Optimize the pulsed field of 1500 V

4.3.1 Examine the limited condition of V_b and T_b

In CE and MCE, high power supply is required for manipulating sample injection and separation electrokinetically (Blanes et al., 2012). In the previous experiments, we verify that the pulsed field can complete the separation with higher SNR over DC field. However, from the electropherogram in Figure 4.3, the distributions of the peaks are not in regulation (Sinton, Ren, & Li, 2003), even the three peaks can be identified. Then, it is necessary to explore the working range for V_b and T_b. An example is investigated that V_f

is 1500 V, but V_b is set to 1200 V with time distribution 300 ms (T_f) and 100 ms (T_b) in Table 4.1.

Table 4. 1 Separation voltage settings for pulsed field in Figure 4.5. (Unit: V)

	S	BW	SW	B
Forward T_f: 300 ms	100	-500	100	1000
Backward T_b : 100 ms	100	1400	100	200

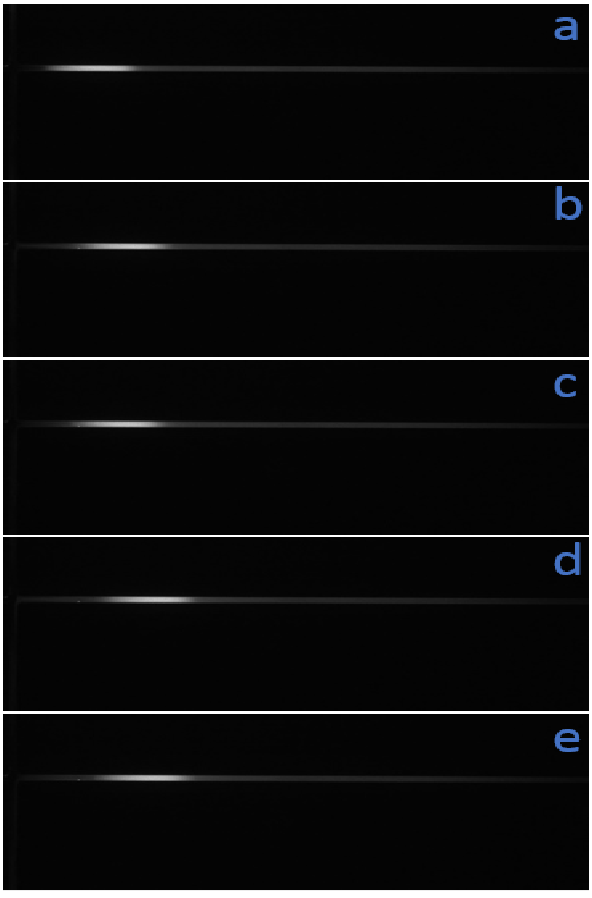

Figure 4. 5 Sample pulg movement under pulsed field V_f : V_b = 1500 V : 1200 V; T_f : T_b = 300 ms : 100 ms. Five consecutive images with an interval time of 0.2 s (Fps 4.72 Hz) under CCD.

The plug is still moving downstream to BW. The five images of the video sequences are showing in Figure 4.5. The plug first is moving forward when V_f is on (Figure 4.5 a-b), and when the direction of electric field changes with V_b on where the plug in Figure 4.5c moves back a little bit. Figure 4.5c-d shows the repeated movement caused by the pulsed field. However, there is no separation occurred under this situation after the sample mixture moves to the edge of the field. We conclude that keep increasing the V_b and T_b may not work well for separation because less time the analytes are taken to migrate with the small voltage difference between V_f and V_b. Also, the longer T_b pushes the sample plug moving back too much that each analyte could not migrate steadily based on its own mobility.

4.3.2 Separation of pulsed field

In the three level of migration speed among 1500 V, 2500 V and 3500 V, 1500 V has a relatively slow migration velocity. If a longer time of V_f is provided, a higher average moving speed may give the chance for separation and minimize the diffusion as well. Accordingly, the V_f 1500 V is remained and the T_f is adjusted to 300 ms instead of 100 ms. V_b and T_b keep the same as 800 V and 50 ms in Table. The electropherogram is shown in Figure 4.6 at two locations of 2.3 mm and 3.3 mm.

As can be seen in Figure 4.6 three analytes are separated in around 15 s at the distance of 2.3 mm. The first peak (RB) is narrow because its migration velocity is faster when passing by the detection point. The other two negatively charged dyes is slower passing by with much wider band. At the location 3.3 mm, a baseline separation of three analytes is achieved.

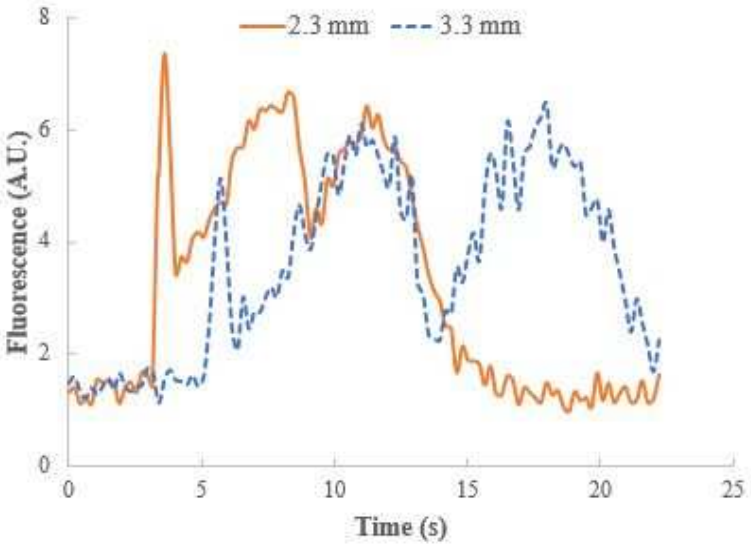

Figure 4. 6 Electropherograms of pulsed field separation at the detection points 2.3 mm and 3.3 mm. Voltage condition V_f : V_b = 1500 V : 800 V; T_f : T_b = 300 ms : 50 ms.

Table 4. 2 Separation voltage settings for pulsed field in Figure 4.6. (Unit: V)

	S	**BW**	**SW**	**B**
Forward T_f: 300 ms	100	-500	100	1000
Backward T_b : 50 ms	100	1000	100	200

The neutral dye first passes through the detection point. The second peak is DCF with the charge of negative one and the last one is FL with negative two. The resolution (*R*) is calculated between two adjancent peaks at each location in Table 4.3. At a distance of 2.3 mm, *R* is 1.06 between RB and DCF which is increased to 1.28 at the distance of 3.3 mm. For two negatively charged sample, *R* is from 0.59 to 0.94 which is almost reach to baseline separation.

Table 4. 3 Resolution between two adjacent peaks for the pulsed field separation of 1500 V. Peaks from left to right are rhodamine B (RB), 2,7-Dichlorofluorescein (DCF) and fluorescein (FL) at the detection points of 2.3 mm and 3.3 mm.

Analytes	Resolution at 2.3 mm	Resolution at 3.3 mm
RB	1.06	1.28
DCF	0.59	0.94
FL		

In the Figure 4.6, the reason for the wider bands of two negative dyes compared with the nuetral one is the different velocity passing by the detection point. Based on the requirement of the research, the sample size injected into separation channel may vary. For example, large volume sample stacking method could improve the dection sensitivity, in other word, it will reduce the effective separatioin length which my sacrify the resolution (Sueyoshi, Kitagawa, & Otsuka, 2008). Since our main focus is not diffusion, the purpose of the experiment is to verify that better separation could be achieved by changing the parameter of the pulsed field.

4.3.3 Same time separation between DC and pulsed field

It is well-known that the longer separation length increases the separation efficiency (Molho et al., 2001). During the same time, the sample in DC field will migrate longer than pulsed field. Then, we compare the separation efficiency for the same traveling time. The aim is to eliminate the bias that the better separation is caused by

longer separation time in pulsed field. Because the analytes in the DC field move fast, the dection point for DC field is at 4.2 mm. The detection point for pulsed field is 1.9 mm. Figure 4.7 is the electropherogram of separation under DC and pulsed field during the same migration time. The arrows indicate the peak for each analyte.

The first peak in pulsed field is high because the detection point is close to intersection where the concentration of the injected sample plug is not decreased yet. In DC field, the whole plug quickly moves to the detection point where the negatively charged dyes are not quite separated that results in the high peak for FL.

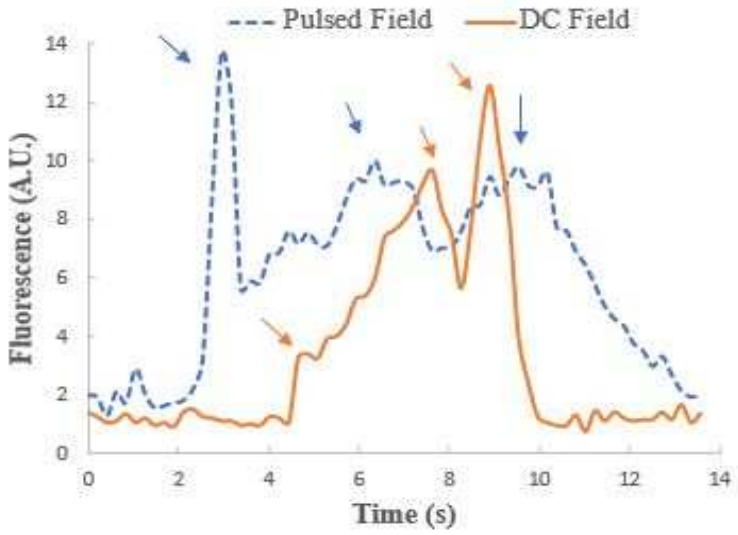

Figure 4. 7 Separation between pulsed and DC field with the same migration time. The detection points are 1.8 mm and 4.2 mm away from the intersection, respectively. The arrows show the peaks.

4.4 Optimize pulsed field of 2500 V

In the case of 2500 V voltage separation, V_b = 600 V is employed. Two sets of time ratio (T_r) are investigated. One is with T_f = 100 ms and T_b = 50 ms (T_r = 2:1); the other one is with T_f = 200 ms and T_b = 50 ms (T_r = 4:1). The applied voltage is shown in

Table 4.4. The electropherograms of separation are presented in Figure 4.8 at the distance of 3 mm away from the intersection for both cases.

Figure 4.8 clearly shows the difference of the migration time in around 12 s and 16 s under the two pulsed time schemes. Longer T_f will result in faster movement that less diffusion contributes to the band broadening. The wider w_{hi} (peak width at the half height of the peak) may cause the loss of the resolution. From the Table 4.5, it proves that the resolution between DCF and FL with T_r = 4:1 is higher than the one with T_r = 2:1 as expected.

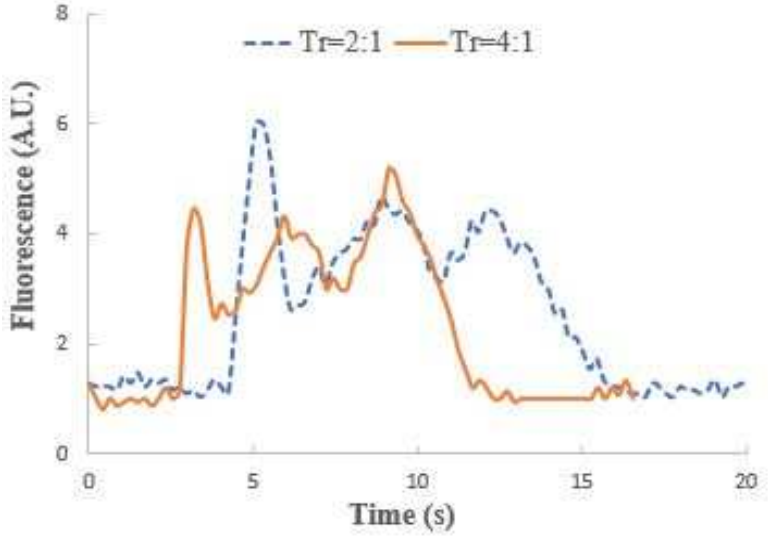

Figure 4. 8 Pulsed field separation under T_r = 2:1 and T_r = 4:1 at detection point of 3 mm along the channel. Separation voltage: V_f = 2500 V; V_b = 600 V.

Table 4. 4 Separation voltage settings for pulsed field in Figure 4.8. (Unit: V)

	S	BW	SW	B
Forward T_f: 100 ms 200 ms	100	-500	100	2000
Backward T_b : 50 ms	100	800	100	200

Table 4. 5 Resolution of the analysis for the pulsed field separation of voltage 2500 V.

Analytes	2500 V, 600 V 100 : 50 ms	2500 V, 600 V 200 : 50 ms
	3.0 mm	3.0 mm
RB	1.00	1.01
DCF	0.73	0.77
FL		

4.5 Optimize pulsed field of 3500 V

The attempt of optimization of 3500 V is employed with the condition shown in Table 4.6.

Table 4. 6 Separation voltage settings for pulsed field in Figure 4.9. (Unit: V)

	S	BW	SW	B
Forward T_f: 300 ms	100	-500	100	3000
Backward T_b : 50 ms	100	1000	100	200

For the voltage of 3500 V, three identified peaks are still available in Figure 4.9. However, the whole separation process is very fast in around 5 s even the V_b is applied. The quick average migration velocity does not allow the analytes to have enough residence time for the improvement of the resolution. Meanwhile, the large external electric field creates high velocity to form a parabolic flow patter. Then the sample will

dilute due to the combination of diffusion, Taylor dispersion and convection, which also can be the explaination of fast decreasing of SNR in Figure 4.4c.

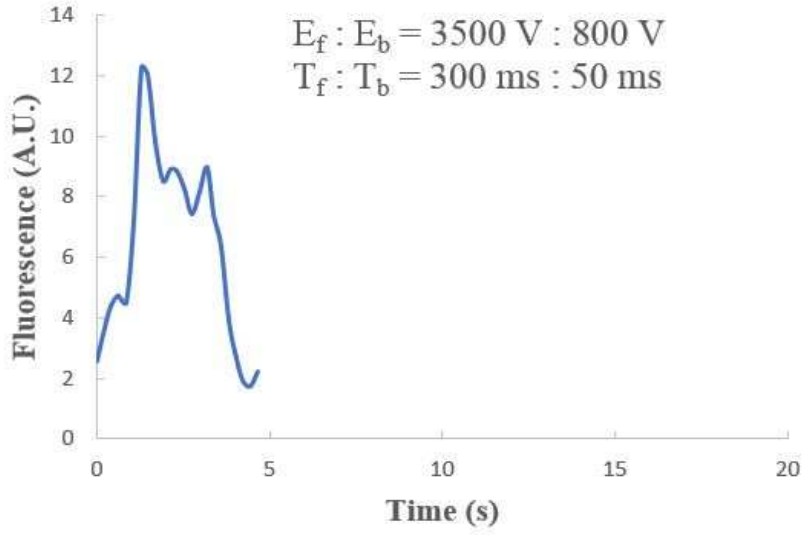

Figure 4. 9 Separation of pulsed field with condition $V_f : V_b$ = 1500 V : 800 V; $T_f : T_b$ = 300 ms : 50 ms.

4.6 Sample stacking

In the case of sample stacking, the analytes used are 13 μM FL (-2) and 15 μM RB (0). As mentioned above, this stacking mode is to concentrate anion species by manipulating the conductivity difference between sample and buffer. Figure 4.10 shows the separation of two fluorescent dyes under DC and puled field. Also, the method of sample stacking is compared with the two situations. In pulsed field (Figure 4.10a-b), the fluorescent intensity of RB in both figures is very close, but there are almost 4-fold enrichment of the intensity for FL.

Compared with the case of sample stacking, the FL highest intensity is 40.3 in pulsed field and 32.3 in DC field. There are 25% increasing with the application of pulsed field. And, we can see the two peaks but there is only one peak in DC. The

possible reason may be that small volume of RB is injected into separation channel and it is diluted by the dispersion. Another one is that blue light is not the best excitation source for RB, the low concentration with small volume make it difficult to detect (Sinton, Ren, Xuan, et al., 2003).

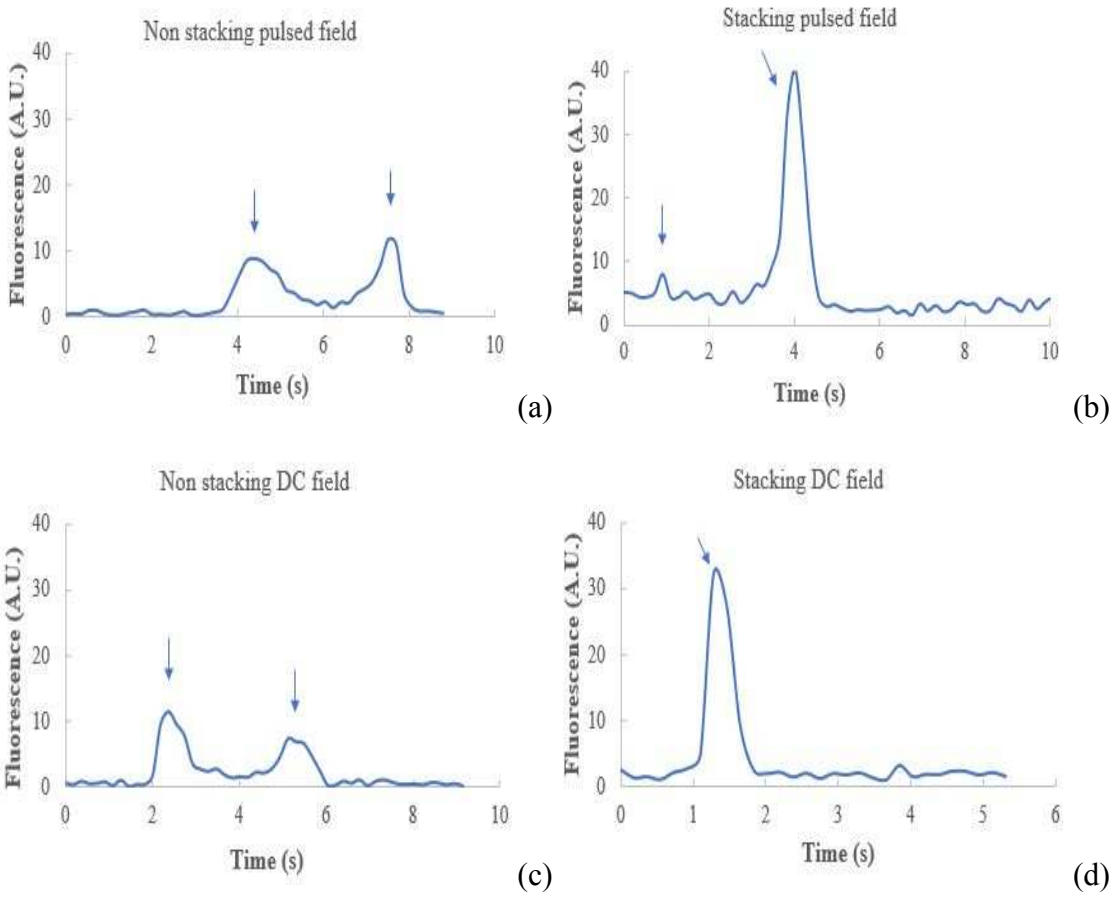

Figure 4. 10 Electropherogram on the separation of two dyes under pulsed field: (a) without stacking; (b)with stacking and under DC field: (c) without stacking and (d)with stacking. The arrows indicate peaks from left (RB) to right (FL).

CHAPTER 5

CONCLUSION

MCE has shown the capability of being the alternative analytical system with many outstanding performances compared with the traditional CE. Fast, money economic, high throughput and easily integrated multiple steps in one system are already demonstrated as the features in the way to the μ-TAS. Many applications in CE have been transferred to a microchip. Numerous approaches are studied to overcome the problems occurring in miniaturized system. For example, the injection process and sample stacking are quite different in the operation in capillary because of the change of geometry. The great efforts on the fundamental study of MCE are still necessary to work on.

The modification of EOF is an approach which was studied to improve the poorly separation in CE. Due to the short effective separation length in miniaturized microchip, the idea of using pulsed field in one aspect is to increase the residence time that the sample can experience longer migration time than DC field. Another aspect is to take advantage of charge-to-mass ratio of the charged analytes by changing the direction of electric field where the analyte will have different reaction time in the way of migration. Eventually, each analyte could be separated with the interval time on their own average velocity.

In our experiments, three different levels of DC voltage first apply to the microchannel as the comparison. The lowest voltage shows the separation of the three

analytes. In contrast, all three pulsed field can complete the separation. To improve the resolution, different pulsed time on each level are investigated. The pulsed field with forward voltage 1500 V and 2500 V gives the better results than 3500 V, which is examined that higher voltage with larger EOF and short separation time may tradeoff the difference of electrophoretic mobility. Also, the SNR in longer separation time for pulsed field will not drop as much as the one in DC field in this domain. In the case of sample stacking, the pulsed field not only shows the ability of separation but a higher SNR over DC field which could be considered as a general power supply option in the area of separation. To the best of our knowledge, this is the first time to apply pulsed field to reach better separation in a size-limited microchip with short effective separation length.

REFERENCES

Alarie, J. P., Jacobson, S. C., Culbertson, C. T., & Ramsey, J. M. (2000). Effects of the electric field distribution on microchip valving performance General, 100–106.

Alarie, J. P., Jacobson, S. C., & Michael Ramsey, J. (2001). Electrophoretic injection bias in a microchip valving scheme. *Electrophoresis*, *22*(2), 312–317. https://doi.org/10.1002/1522-2683(200101)22:2<312::AID-ELPS312>3.0.CO;2-3

Backhouse, C. J., Gajdal, A., Pilarski, L. M., & Crabtree, H. J. (2003). Improved resolution with microchip-based enhanced field inversion electrophoresis. *Electrophoresis*, *24*(11), 1777–1786. https://doi.org/10.1002/elps.200305398

Barker, S. L. R., Ross, D., Tarlov, M. J., Gaitan, M., & Locascio, L. E. (2000). Control of Flow Direction in Microfluidic Devices with Polyelectrolyte Multilayers, *72*(24), 5925–5929. https://doi.org/10.1021/ac0008690

Beckers, J. L., & Bocek, P. (2000). Sample stacking in capillary zone elctrophoresis: Principles, advantages and limitations. *Electrophoresis*, *21*, 2747–2767.

Belder, D., Deege, A., Kohler, F., & Ludwig, M. (2002). Poly(vinyl alcohol)-coated microfluidic devices for high-performance microchip electrophoresis. *Electrophoresis*, *23*(20), 3567–3573. https://doi.org/10.1002/1522-2683(200210)23:20<3567::AID-ELPS3567>3.0.CO;2-3

Belder, D., & Ludwig, M. (2003). Surface modification in microchip electrophoresis.

Bharadwaj, R., & Santiago, J. G. (2005). Dynamics of field-amplified sample stacking. *Journal of Fluid Mechanics*, *543*, 57–92. https://doi.org/10.1017/S0022112005005975

Bharadwaj, R., Santiago, J. G., & Mohammadi, B. (2002). Design and optimization of on-chip capillary electrophoresis. *Electrophoresis*, *23*(16), 2729–2744. https://doi.org/10.1002/1522-2683(200208)23:16<2729::AID-ELPS2729>3.0.CO;2-I

Birrer, B. W., Simon, M. I., & Lai, E. (1990). The basis of high resolution separation of small DNAs by asymmetric-voltage field inversion electrophoresis and its application to DNA sequencing gels. *Nucleic Acids Research*, *18*(6), 1481–1487. https://doi.org/10.1093/nar/18.6.1481

Blanes, L., Coltro, W. K. T., Saito, R. M., Van Gramberg, A., Lucio do Lago, C., & Doble, P. (2012). High-voltage power supplies to capillary and microchip electrophoresis. *Electrophoresis*, *33*(6), 893–898. https://doi.org/10.1002/elps.201100490

Blas, M., Delaunay, N., Ferrigno, R., & Rocca, J. L. (2007). Numerical simulations of the second-order electrokinetic bias observed with the gated injection mode in chips. *Electrophoresis*, *28*(17), 2961–2970. https://doi.org/10.1002/elps.200600692

Blas, M., Delaunay, N., & Rocca, J.-L. (2008). Electrokinetic-based injection modes for separative microsystems. *Electrophoresis*, *29*(1), 20–32. https://doi.org/10.1002/elps.200700389

Breadmore, M. C. (2012). Capillary and microchipE challenging the common conceptions.pdf. *Journal of Chromatography A*, *1221*, 42–55.
Bruin, G. J. M. (2000). Recent developments in electrokinetically driven analysis on microfabricated devices. *Electrophoresis*. https://doi.org/10.1002/1522-2683(200012)21:18<3931::AID-ELPS3931>3.0.CO;2-M
Buchholz, B. A., Huiberts, P. J., Stein, T. M., & Barron, A. E. (2002). A novel , hydrophilic , self-coating polymer matrix for DNA sequencing by capillary electrophoresis, 1429–1440.
Büttgenbach, S., & Wilke, R. (2005). A capillary electrophoresis chip with hydrodynamic sample injection for measurements from a continuous sample flow. *Analytical and Bioanalytical Chemistry*, *383*(5), 733–737. https://doi.org/10.1007/s00216-005-3346-6
Carle, G. F., & Olson, M. V. (1984). Separation of chromosomal DNA molecules from yeast by orthogonal-field-alternation gel electrophoresis. *Nucleic Acids Research*, *12*. https://doi.org/10.1093/nar/16.5.2269
Chan, A. S., Danquah, M. K., Agyei, D., Hartley, P. G., & Zhu, Y. (2014). A simple microfluidic chip design for fundamental bioseparation. *Journal of Analytical Methods in Chemistry*, *2014*. https://doi.org/10.1155/2014/175457
Chen, G., Lin, Y., & Wang, J. (2006). Microchip capillary electrophoresis with electrochemical detection for monitoring environmental pollutants. *Current Analytical Chemistry*, *2*(1), 8932–8936. https://doi.org/10.2174/157341106775197439
Chen, P., Feng, X., Sun, J., Wang, Y., Du, W., & Liu, B.-F. (2010). Hydrodynamic gating for sample introduction on a microfluidic chip. *Lab on a Chip*, *10*(11), 1472–1475. https://doi.org/10.1039/b925096d
Cifuentes, A. (2006). Recent advances in the application of capillary electromigration methods for food analysis. *Electrophoresis*, *27*(1), 283–303. https://doi.org/10.1002/elps.200500474
Colyer, C. L., Mangru, S. D., & Harrison, D. J. (1997). Microchip-based capillary electrophoresis of human serum proteins. *Journal of Chromatography. A*, *781*(1–2), 271–276.
Dolnik, V., & Liu, S. (2005). Applications of capillary electrophoresis on microchip. *Journal of Separation Science*. https://doi.org/10.1002/jssc.200500243
Dolník, V., Liu, S., & Jovanovich, S. (2000). Capillary electrophoresis on microchip CE and CEC. *Electrophoresis*, (21), 41–54.
Duffy, D. C., McDonald, J. C., Schueller, O. J. A., & Whitesides, G. M. (1998). Rapid prototyping of microfluidic systems in poly(dimethylsiloxane). *Analytical Chemistry*, *70*(23), 4974–4984. https://doi.org/10.1021/ac980656z
Dunsmoor, C., Sanders, J., Ferrance, J., & Et Al. (2001). Microchip Electrophoresis : An Emerging Technology for Molecular Diagnostics. *LC GC Europe*, (January), 38–44.
Ermakov, S. V., Jacobson, S. C., & Ramsey, J. M. (2000). Computer simulations of electrokinetic injection techniques in microfluidic devices. *Analytical Chemistry*, *72*(15), 3512–3517. https://doi.org/10.1021/ac991474n
Gao, J., Yin, X.-F., & Fang, Z.-L. (2004). Integration of single cell injection, cell lysis, separation and detection of intracellular constituents on a microfluidic chip. *Lab on a Chip*, *4*(1), 47–52. https://doi.org/10.1039/b310552k

Giordano, B. C., Burgi, D. S., Hart, S. J., & Terray, A. (2012). On-line sample pre-concentration in microfluidic devices : A review. *Analytica Chimica Acta*, *718*, 11–24. https://doi.org/10.1016/j.aca.2011.12.050

Gong, M., Wehmeyer, K. R., Stalcup, A. M., Limbach, P. A., & Heineman, W. R. (2007). Study of injection bias in a simple hydrodynamic injection in microchip CE. *Electrophoresis*, *28*(10), 1564–1571. https://doi.org/10.1002/elps.200600616

Han, J., & Singh, A. K. (2004). Rapid protein separations in ultra-short microchannels: Microchip sodium dodecyl sulfate-polyacrylamide gel electrophoresis and isoelectric focusing. *Journal of Chromatography A*, *1049*(1–2), 205–209. https://doi.org/10.1016/j.chroma.2004.08.018

Harrison, D. J., Manz, A., Fan, Z., Luedi, H., & Widmer, H. M. (1992). Capillary electrophoresis and sample injection systems integrated on a planar glass chip. *Analytical Chemistry*, *64*(20), 1926–1932. https://doi.org/10.1021/ac00041a030

Haswell, S. J. (1997). Critical Review Development and Operating Characteristics of Micro Flow Injection Analysis Systems Based on Electroosmotic Flow, *122*(January), 6–8.

Herrera-Herrera, A. V., Ravelo-Pérez, L. M., Hernández-Borges, J., Afonso, M. M., Palenzuela, J. A., & Rodríguez-Delgado, M. Á. (2011). Oxidized multi-walled carbon nanotubes for the dispersive solid-phase extraction of quinolone antibiotics from water samples using capillary electrophoresis and large volume sample stacking with polarity switching. *Journal of Chromatography A*, *1218*(31), 5352–5361. https://doi.org/10.1016/j.chroma.2011.06.031

Hu, S., Ren, X., Bachman, M., Sims, C. E., Li, G. P., & Allbritton, N. (2003). Cross-linked coatings for electrophoretic separations in poly(dimethylsiloxane) microchannels. *Electrophoresis*, *24*(21), 3679–3688. https://doi.org/10.1002/elps.200305592

Huang, F.-C., Liao, C.-S., & Lee, G.-B. (2006). An integrated microfluidic chip for DNA/RNA amplification, electrophoresis separation and on-line optical detection. *Electrophoresis*, *27*(16), 3297–3305. https://doi.org/10.1002/elps.200600458

Huang, W. H., Ai, F., Wang, Z. L., & Cheng, J. K. (2008). Recent advances in single-cell analysis using capillary electrophoresis and microfluidic devices. *Journal of Chromatography B: Analytical Technologies in the Biomedical and Life Sciences*, *866*(1–2), 104–122. https://doi.org/10.1016/j.jchromb.2008.01.030

Jacobson, S. C., Culbertson, C. T., Daler, J. E., & Ramsey, J. M. (1998). Microchip Structures for Submillisecond, *70*(16), 3476–3480. https://doi.org/10.1021/ac980349t

Jacobson, S. C., Hergenroder, R., Koutny, L. B., Warmack, R. J., & Ramsey, J. M. (1994). Effects of Injection Schemes and Column Geometry on the Performance of Microchip Electrophoresis Devices. *Analytical Chemistry*, *66*(123), 1107–1113. https://doi.org/10.1021/ac00079a028

Jacobson, S. C., Moore, A. W., & Ramsey, J. M. (1995). Fused quartz substrates for microchip electrophoresis. *Anal. Chem.*, *67*(13), 2059–2063. https://doi.org/10.1021/ac00109a026

Jena, R. K., & Yue, C. Y. (2012). Cyclic olefin copolymer based microfluidic devices for biochip applications: Ultraviolet surface grafting using 2-methacryloyloxyethyl phosphorylcholine. *Biomicrofluidics*, *6*(1), 1–12. https://doi.org/10.1063/1.3682098

Jin, S., Anderson, G. J., & Kennedy, R. T. (2013). Western blotting using microchip electrophoresis interfaced to a protein capture membrane. *Analytical Chemistry*, *85*(12), 6073–6079. https://doi.org/10.1021/ac400940x

Kar, S., & Dasgupta, P. K. (1999). Improving resolution in capillary zone electrophoresis through bulk flow control. *Microchemical Journal*, *62*(1), 128–137. https://doi.org/10.1006/mchj.1999.1718

Karlinsey, J. M. (2012). Sample introduction techniques for microchip electrophoresis : A review. *Analytica Chimica Acta*, *725*, 1–13. https://doi.org/10.1016/j.aca.2012.02.052

Karlinsey, J. M., Monahan, J., Marchiarullo, D. J., Ferrance, J. P., & Landers, J. P. (2005). Pressure injection on a valved microdevice for electrophoretic analysis of submicroliter samples. *Analytical Chemistry*, *77*(11), 3637–3643. https://doi.org/10.1021/ac048115z

Kim, M. S., Cho, S. Il, Lee, K. N., & Kim, Y. K. (2005). Fabrication of microchip electrophoresis devices and effects of channel surface properties on separation efficiency. *Sensors and Actuators, B: Chemical*, *107*(2), 818–824. https://doi.org/10.1016/j.snb.2004.12.069

Köhler, S., Benz, C., Becker, H., Beckert, E., Beushausen, V., & Belder, D. (2012). Micro free-flow electrophoresis with injection molded chips. *RSC Adv.*, *2*(2), 520–525. https://doi.org/10.1039/C1RA00874A

Kutter, J. örg P. (2000). Current developments in electrophoretic and chromatographic separation methods on microfabricated devices. *TrAC - Trends in Analytical Chemistry*, *19*(6), 352–363. https://doi.org/10.1016/S0165-9936(00)00014-5

Lee, C. L. J. H. G., & Mems, M. Á. L. Á. (2011). Sample preconcentration in microfluidic devices, 481–511. https://doi.org/10.1007/s10404-010-0661-9

Lin, C.-H., Wang, J.-H., & Fu, L.-M. (2008). Improving the separation efficiency of DNA biosamples in capillary electrophoresis microchips using high-voltage pulsed DC electric fields. *Microfluidics and Nanofluidics*, *5*(3), 403–410. https://doi.org/10.1007/s10404-008-0259-7

Liu, J., & Lee, M. L. (2006). Permanent surface modification of polymeric capillary electrophoresis microchips for protein and peptide analysis. *Electrophoresis*. https://doi.org/10.1002/elps.200600082

Llopis, S. L., Osiri, J., & Soper, S. A. (2007). Surface modification of poly(methyl methacrylate) microfluidic devices for high-resolution separations of single-stranded DNA. *Electrophoresis*, *28*(6), 984–993. https://doi.org/10.1002/elps.200600435

Lu, H., Koo, L. Y., Wang, W. M., Lauffenburger, D. A., Griffith, L. G., & Jensen, K. F. (2004). Microfluidic Shear Devices for Quantitative Analysis of Cell Adhesion, *76*(18), 5257–5264. https://doi.org/10.1021/ac049837t

Manz, A., Graber, N., & Widmer, H. M. (1990). Miniaturized total chemical analysis systems: A novel concept for chemical sensing. *Sensors and Actuators B: Chemical*, *1*(1–6), 244–248. https://doi.org/10.1016/0925-4005(90)80209-I

McDonald, J. C., Duffy, D. C., Anderson, J. R., Chiu, D. T., Wu, H., Schueller, O. J. A., & Whitesides, G. M. (2000). fabrication of microfluidics in poly(dimethylsiloxane).pdf. *Electrophoresis2*, *21*, 27–40.

Milanova, D., Chambers, R. D., Bahga, S. S., & Santiago, J. G. (2011). Electrophoretic mobility measurements of fluorescent dyes using on-chip capillary electrophoresis.

Electrophoresis, *32*(22), 3286–3294. https://doi.org/10.1002/elps.201100210
Molho, J. I., Herr, A. E., Mosier, B. P., Santiago, J. G., Kenny, T. W., Brennen, R. A., … Mohammadi, B. (2001). Optimization of turn geometries for microchip electrophoresis. *Analytical Chemistry*, *73*(6), 1350–1360. https://doi.org/10.1021/ac001127+
Nuchtavorn, N., Smejkal, P., Breadmore, M. C., Guijt, R. M., Doble, P., Bek, F., … Macka, M. (2013). Exploring chip-capillary electrophoresis-laser-induced fluorescence field-deployable platform flexibility: separations of fluorescent dyes by chip-based non-aqueous capillary electrophoresis. *Journal of Chromatography. A*, *1286*, 216–221. https://doi.org/10.1016/j.chroma.2013.02.060
Nuchtavorn, N., Suntornsuk, W., Lunte, S. M., & Suntornsuk, L. (2015). Recent applications of microchip electrophoresis to biomedical analysis. *Journal of Pharmaceutical and Biomedical Analysis*. https://doi.org/10.1016/j.jpba.2015.03.002
Oleschuk, R. D., & Harrison, D. J. (2003). Microchip-based capillary electrochromatography, 3018–3025. https://doi.org/10.1002/elps.200305538
Palmer, J., Burgi, D. S., Munro, N. J., & Landers, J. P. (2001). Electrokinetic injection for stacking neutral analytes in capillary and microchip electrophoresis. *Analytical Chemistry*, *73*(4), 725–731. https://doi.org/10.1021/ac001046d
Perez-Ruiz, T., Martinez-Lozano, C., Sanz, A., & Bravo, E. (1998). Separation of fluorescein dyes by capillary electrophoresis using beta-cyclodextrin. *Chromatographia*, *48*(3–4), 263–267.
Preisler, J., & Yeung, E. S. (1996). Characterization of Nonbonded Poly (ethylene oxide) Coating for Capillary Electrophoresis via Continuous Monitoring of Electroosmotic Flow, *68*(17), 2885–2889. https://doi.org/10.1021/ac960260s
Pumera, M. (2006). Analysis of explosives via microchip electrophoresis and conventional capillary electrophoresis: A review. *Electrophoresis*. https://doi.org/10.1002/elps.200500609
Reyes, D. R., Iossifidis, D., Auroux, P.-A., & Manz, A. (2002). Micro total analysis systems. 1. Introduction, theory, and technology. *Analytical Chemistry*. https://doi.org/10.1021/ac0202435
Ríos, Á., Zougagh, M., & Avila, M. (2012). Miniaturization through lab-on-a-chip: Utopia or reality for routine laboratories? A review. *Analytica Chimica Acta*. https://doi.org/10.1016/j.aca.2012.06.024
Roy, S., Das, T., & Yue, C. Y. (2013). High performance of cyclic olefin copolymer-based capillary electrophoretic chips. *ACS Applied Materials and Interfaces*, *5*(12), 5683–5689. https://doi.org/10.1021/am401081d
Schwartz, D. C., & Cantor, C. R. (1984). Separation of yeast chromosome-sized DNAs by pulsed field gradient gel electrophoresis. *Cell*, *37*(1), 67–75. https://doi.org/10.1016/0092-8674(84)90301-5
Shultz-Lockyear, L. L., Colyer, C. L., Fan, Z. H., Roy, K. I., & Harrison, D. J. (1999). Effects of injector geometry and sample matrix on injection and sample loading in integrated capillary electrophoresis devices. *Electrophoresis*, *20*(3), 529–538. https://doi.org/10.1002/(SICI)1522-2683(19990301)20:3<529::AID-ELPS529>3.0.CO;2-7
Sinton, D., Ren, L., & Li, D. (2003). Visualization and numerical modelling of

microfluidic on-chip injection processes. *Journal of Colloid and Interface Science*, *260*(2), 431–439. https://doi.org/10.1016/S0021-9797(02)00181-9

Sinton, D., Ren, L., Xuan, X., & Li, D. (2003). Effects of liquid conductivity differences on multi-component sample injection, pumping and stacking in microfluidic chips. *Lab on a Chip*, *3*(3), 173–179. https://doi.org/10.1039/b304614a

Soliva-Fortuny, R., Balasa, A., Knorr, D., & Martín-Belloso, O. (2009). Effects of Pulsed Electric Fields on Bioactive Compounds in Foods: A Review. *Trends in Food Science & Technology*, *20*(11–12), 544–556. https://doi.org/10.1016/j.tifs.2009.07.003

Sueyoshi, K., Kitagawa, F., & Otsuka, K. (2008). Review Recent progress of online sample preconcentration techniques in microchip electrophoresis, 2650–2666. https://doi.org/10.1002/jssc.200800272

Tabuchi, M., Kuramitsu, Y., Nakamura, K., & Baba, Y. (2003). A 15-s protein separation employing hydrodynamic force on a microchip. *Analytical Chemistry*, *75*(15), 3799–3805. https://doi.org/10.1021/ac030051p

Takayama, S., Ostuni, E., Leduc, P., Naruse, K., Ingber, D. E., & Whitesides, G. M. (2003). Selective Chemical Treatment of Cellular Microdomains Using Multiple Laminar Streams, *10*, 123–130. https://doi.org/10.1016/S

Tiselius, A. (1937). A new apparatus for electrophoretic analysis of colloidal mixtures. *Transactions of the Faraday Society*, *33*, 524. https://doi.org/10.1039/tf9373300524

Ueda, M., Endo, Y., Abe, H., Kuyama, H., Nakanishi, H., Arai, A., & Baba, Y. (2001). Field-inversion electrophoresis on a microchip device. *Electrophoresis*, *22*(2), 217–221. https://doi.org/10.1002/1522-2683(200101)22:2<217::AID-ELPS217>3.0.CO;2-O

Verpoorte, E. (2002). Microfluidic chips for clinical and forensic analysis. *Electrophoresis*. https://doi.org/10.1002/1522-2683(200203)23:5<677::AID-ELPS677>3.0.CO;2-8

Vickers, J. A., & Henry, C. S. (2005). Simplified current decoupler for microchip capillary electrophoresis with electrochemical and pulsed amperometric detection. *Electrophoresis*, *26*(24), 4641–4647. https://doi.org/10.1002/elps.200500508

Wang, J., Pumera, M., Chatrathi, M. P., Escarpa, A., Konrad, R., Griebel, A., … Löwe, H. (2002). Towards disposable lab-on-a-chip : Poly (methylmethacrylate) microchip electrophoresis device with electrochemical detection, 596–601.

Whitesides, G. M. (2006). The origins and the future of microfluidics. *Nature*, *442*(7101), 368–373. https://doi.org/10.1038/nature05058

Wuethrich, A., & Quirino, J. P. (2017). Sensitivity enhancing injection from a sample reservoir and channel interface in microchip electrophoresis. *Journal of Separation Science*, *40*(4), 927–932. https://doi.org/10.1002/jssc.201601064

Yin, X.-B., & Wang, E. (2005). Capillary electrophoresis coupling with electrochemiluminescence detection: a review. *Analytica Chimica Acta*, *533*(2), 113–120. https://doi.org/10.1016/j.aca.2004.11.015

You, A., Be, M. A. Y., & In, I. (2011). The effect of an external electric field on diffusion-controlled bulk ion recombination, *5874*(December 1993). https://doi.org/10.1063/1.467099

Zhang, J., Das, C., & Fan, H. Z. (2008). Dynamic coating for protein separation in cyclic olefin copolymer microfluidic devices. *Microfluidics and Nanofluidics*, *5*(3), 327–

335. https://doi.org/10.1007/s10404-007-0253-5
Zhang, L., Yin, X., & Fang, Z. (2006). Negative pressure pinched sample injection for microchip-based electrophoresis. *Lab on a Chip*, *6*(2), 258–264. https://doi.org/10.1039/b511924c